Enisamium is a small molecule inhibitor of the influenza A virus and SARS-CoV-2 RNA polymerases

Alexander P Walker[1,5], Haitian Fan[1], Jeremy R Keown[2], Victor Margitich[3], Jonathan M Grimes[2], Ervin Fodor[1*] and Aartjan J W te Velthuis[4,5*]

[1]Sir William Dunn School of Pathology, University of Oxford, South Parks Road, OX1 3RE, United Kingdom

[2]Division of Structural Biology, Henry Wellcome Building for Genomic Medicine, University of Oxford, OX3 7BN, United Kingdom

[3]Farmak Public Joint Stock Company, Kyrylivska Street, 04080, Ukraine

[4]Division of Virology, Department of Pathology, Addenbrooke's Hospital, University of Cambridge, Hills Road, CB2 2QQ, United Kingdom

[5]These authors contributed equally: Alexander P Walker, Aartjan J W te Velthuis

[*]email: ervin.fodor@path.ox.ac.uk, ajwt6@cam.ac.uk

Abstract

Influenza A virus and coronavirus strains cause a mild to severe respiratory disease that can result in death. Although vaccines exist against circulating influenza A viruses, such vaccines are ineffective against emerging pandemic influenza A viruses. Currently, no vaccine exists against coronavirus infections, including pandemic SARS-CoV-2, the causative agent of the Coronavirus Disease 2019 (COVID-19). To combat these RNA virus infections, alternative antiviral strategies are needed. A key drug target is the viral RNA polymerase, which is responsible for viral RNA synthesis. In January 2020, the World Health Organisation identified enisamium as a candidate therapeutic against SARS-CoV-2. Enisamium is an isonicotinic acid derivative that is an inhibitor of multiple influenza B and A virus strains in cell culture and clinically approved in 11 countries. Here we show using *in vitro* assays that enisamium and its putative metabolite, VR17-04, inhibit the activity of both the influenza virus RNA polymerase as well as the SARS-CoV-2 RNA polymerase complex. These results suggest that enisamium is a broad-spectrum small molecule inhibitor of RNA virus RNA synthesis, and implicate it as a possible therapeutic option for treating SARS-CoV-2 infection.

Introduction

RNA viruses, such as pandemic H1N1 influenza A virus (IAV) and severe acute respiratory coronavirus 2 (SARS-COV-2), are among the most important human pathogens. While IAV and SARS-CoV-2 are different viruses and follow different replication cycles, both can cause severe respiratory disease in humans that leads to high morbidity and mortality. Vaccines exist against influenza viruses; however, long vaccine development times mean that antigenic mismatches can occur between circulating influenza virus strains and the vaccine strain. Moreover, due to antigenic shift, existing vaccines are not effective against emerging pandemic influenza viruses(1). No vaccine currently exists against coronaviruses, including the SARS-CoV-2 pandemic and SARS-CoV epidemic strains, which cause Coronavirus Disease 2019 (Covid-19) and SARS respectively. Therefore, research is

needed into conserved viral enzymatic activities, such as RNA polymerase activity, which could be targeted by broad spectrum antivirals(2, 3).

IAVs are negative sense RNA viruses whose 14 kb genome consists of eight segments of single-stranded viral RNA (vRNA). The viral RNA-dependent RNA polymerase (FluPol) copies the vRNA into a replicative intermediate called the complementary RNA (cRNA) during viral replication, or into capped and polyadenylated viral messenger RNA (mRNA) during viral transcription(4, 5). The cRNA serves as a template for the production of new vRNA molecules. vRNA and cRNA molecules are both replicated in the context of ribonucleoproteins (RNPs), which consist of FluPol bound to the 5' and 3' ends of a genome segment and the rest of the vRNA or cRNA is bound by a helical coil of nucleoprotein (NP). FluPol is composed of three subunits: polymerase basic 1 (PB1), PB2, and polymerase acidic (PA). Structural analyses have shown that the PB1 subunit adopts canonical right hand-like fold, which contains the fingers, palm and thumb subdomains that are conserved among all RNA polymerases. The PA subunit has a large C-terminal domain that is integrated into the PB1 thumb subdomain, and is connected to an N-terminal endonuclease domain by a flexible linker. The PB2 subunit is composed of several globular domains, including cap binding and 627 domains, which are flexible with respect to the core PB1 subunit(4).

SARS-CoV-2 is a betacoronavirus in the order Nidovirales, and has a positive-sense, non-segmented RNA genome of around 30 kilobases(2, 6). The viral genome has a 5' 7-methylguanosine (m^7G) cap and 3' poly(A) tail, modifications which allow the viral genome to be translated by cellular machinery. Two-thirds of the viral genome is made up of two overlapping open reading frames (ORFs), 1a and 1b, which are translated into two large polyproteins immediately upon infection. The two polyproteins are cleaved by intrinsic proteolytic activity to produce non-structural proteins (nsps) 1-16, which collectively form the membrane-associated replication-transcription complex (RTC). The RTC has several major functions: Firstly, it synthesises full-length negative-sense viral RNAs, which are the templates for new positive-sense viral RNA genomes. Secondly, it synthesises subgenomic negative-sense viral RNAs which contain the ribosome-accessible ORFs of structural and accessory proteins. Finally, the RTC transcribes subgenomic or full-length negative-sense viral RNAs into 5' m^7G capped, 3' polyadenylated viral mRNAs. The multiple functions of the replicase complex requires nsp1-16 to have many catalytic activities, such as m^7G cap synthesis, which are not entirely understood(7).

Nsp12 is the RNA-dependent RNA polymerase component of the replicase complex, and it requires nsp7 and nsp8 for processivity(8, 9). The structures of nsp7/8/12 complexes from SARS-CoV and SARS-CoV-2 have been solved by cryo-EM(10, 11). Nsp12 is the core of the complex that adopts the canonical right-handed RNA polymerase fold that is flanked by an N-terminal domain previously linked to nucleotidyltransferase activity(12). One nsp7 and two nsp8 molecules form a complex with each nsp12, and these have been suggested to promote RNA binding by stabilising the nsp12 fingers domain.

IAV FluPol and CoV RTC are important drug targets. However, due to the SARS-CoV-2 RTC possessing error correcting exonuclease activity, the potential susceptibility of nsp12 to existing nucleoside analogues may not be sufficient to inhibit the SARS-CoV-2 RTC(13). Remdesivir has been shown to inhibit the SARS-CoV-2 nsp7/8/12 complex and not be excised by the nsp14 exonuclease, and other nucleoside analogue drugs have been suggested as therapeutic candidates(14, 15). However, there are currently no drugs licensed to treat SARS-CoV-2 infection, or any small molecule inhibitors known that could circumvent the nsp14 exonuclease activity. Enisamium (4-(benzylcarbamoyl)-1-methylpyridinium) iodide (FAV00A), marketed as Amizon®, was highlighted by the World Health Organisation as a candidate therapeutic against SARS-CoV-2(16). Enisamium iodide is licensed for

use in 11 countries including Ukraine and Russia, and has been shown to have clinical efficacy against influenza A and B virus infections(17). It is thought to inhibit influenza virus RNA synthesis, however, the mechanism of action is currently unknown(18).

In this study, we show that enisamium and a putative hydroxylated metabolite, VR17-04, inhibit FluPol activity *in vitro*. Using an *in vitro* activity assay for the SARS-CoV-2 nsp7/8/12 complex, we further show that enisamium and VR17-04 both inhibit SARS-CoV-2 nsp7/8/12 activity during extension of an RNA primer. These data suggest that enisamium is metabolised and directly targets the viral RNA polymerase. The inhibition of RNA synthesis by both IAV and SARS-CoV-2 implies that enisamium is a broad-spectrum small molecule inhibitor of RNA virus RNA synthesis, and is a possible therapeutic option for treating SARS-CoV-2 infection.

Results

Enisamium inhibits FluPol activity in cell culture

Previous experiments showed that enisamium iodide can inhibit influenza virus replication in tissue culture(18). To test if enisamium can inhibit IAV RNA synthesis in a minigenome context, HEK 293T cells were transfected with plasmids expressing FluPol subunits from influenza A/WSN/33 (H1N1) virus (WSN) (pcDNA3-PB1, pcDNA3-PB2, pcDNA3-PA), the viral NP (pcDNA3-NP) and a vRNA template based on segment 5 (NP-encoding genome segment). To estimate the effect of enisamium on host cell RNA synthesis, we transfected a plasmid expressing GFP from a constitutively active CMV promoter. As a further control, we analysed the effect of enisamium on the ribosomal RNA (rRNA) steady state level. After transfection, enisamium was added to the cell culture medium at the concentrations indicated in Fig. 1A. Total cellular RNA was extracted 24 hours post-transfection, and IAV replication (vRNA synthesis) activity was analysed by radioactive primer extension. Enisamium significantly affected IAV replication with an IC_{50} of 354 µM, while our controls showed no significant effect on 5S rRNA or GFP expression levels (Fig. 1A). Overall, these observations suggest that enisamium has no effect on host cell viability, but a direct, differential effect on IAV RNA synthesis.

Enisamium and the putative metabolite VR17-04 inhibit FluPol activity

To examine the effect of enisamium on IAV RNA synthesis *in vitro*, we expressed protein A-tagged WSN IAV FluPol in HEK 293T cells and purified the heterotrimeric complex using IgG sepharose chromatography. We then performed *in vitro* RNA synthesis assays using a model 14 nucleotide (nt) viral RNA (vRNA) template in the presence of different concentrations of enisamium. In these assays, enisamium weakly inhibited FluPol activity with an IC_{50} of 46.3 mM (Fig. 1B, C). This suggests that the inhibitory effect of enisamium on the FluPol activity *in vitro* is limited.

The weak inhibition of FluPol by enisamium is unlikely to be responsible for antiviral efficacy observed in cell culture. To test if a metabolite of enisamium could be a more potent inhibitor of FluPol activity, we treated A549 cells with enisamium for 24 hours and then performed FluPol activity assays in the presence of cellular extract. We observed a strong, concentration-dependent inhibition of FluPol activity, which is consistent with a metabolite of enisamium inhibiting influenza virus RNA synthesis (Fig. 1D). To test if enisamium metabolites have a direct effect on FluPol activity *in vitro*, 9 metabolites were synthesised (Table 1) and titrated in *in vitro* reactions containing purified FluPol. Only hydroxylated metabolite VM17-04 inhibited FluPol activity 55-fold more potently than

enisamium, with an IC_{50} of 840 µM (Fig. 1B, C). Collectively, these data suggest that hydroxylation of enisamium increases the potency against FluPol RNA synthesis *in vitro*.

Enisamium and VM17-04 inhibit SARS-CoV-2 nsp7/8/12 activity

To determine if enisamium and its putative metabolite VR17-04 can inhibit the SARS-CoV-2 replicase complex we developed a SARS-CoV-2 replicase *in vitro* assay that involved nsp12 as the RNA-dependent RNA polymerase, and nsp7 and nsp8 as processivity factors(8). We expressed and purified SARS-CoV-2 nsp7, nsp8 and nsp12, and mixed them at a ratio of 2:2:1 to form a nsp7/8/12 complex (Fig 2A). To test *in vitro* RNA synthesis activity, we incubated the nsp7/8/12 complex with a 40 nt RNA template and a radiolabelled 20 nt RNA primer (Fig 2B, C). The nsp7/8/12 complex was able to extend the 20 nt primer in the presence of NTPs into a doublet of major products of approximately 40 nt in length. This pattern was previously observed for the SARS-CoV nsp7/8/12 complex(8). The proportion of 20 nt primer extended by nsp7/8/12 increased over time, plateauing at around 30 minutes (Fig 2D).

To test the ability of enisamium to inhibit SARS-CoV-2 nsp7/8/12, we performed *in vitro* RNA synthesis assays in the presence of enisamium and the putative metabolite VR17-04 (Fig 3A). Enisamium inhibited nsp7/8/12 activity at relatively high concentrations, with an IC_{50} of 40.7 mM (Fig 3B, C). VR17-04 exhibited over 10-fold more potent inhibition, with an estimated IC_{50} of 2-3 mM. These IC_{50} values are within an order of magnitude of those calculated for the inhibition of FluPol by enisamium and VR17-04. Collectively, these data show that RNA synthesis by the SARS-CoV-2 nsp7/8/12 complex is inhibited by enisamium and its putative metabolite VR17-04.

Discussion

In this study we showed that enisamium and a putative metabolite, VR17-04, inhibit FluPol RNA synthesis activity *in vitro*. We then established an *in vitro* RNA synthesis assay for the nsp7/8/12 complex of SARS-CoV-2, and used this assay to show that enisamium and VM17-04 also inhibit RNA synthesis by SARS-CoV-2 nsp7/8/12.

Our *in vitro* assays indicate that enisamium and VM17-04 inhibit FluPol activity with relatively high IC_{50} values, 46.3 mM and 0.84 mM respectively. However, enisamium strongly inhibits influenza virus growth in cell culture, with EC_{90} values ranging from 157-439 µM(18). This apparent discrepancy may be due to enisamium exerting additional antiviral effects through other mechanisms. In addition, we can currently not exclude that the effect of enisamium is exerted by another, more potent enisamium metabolite. On the other hand, the mechanism of action of the drugs and their efficacy are likely to be highly dependent on the length of the RNA being synthesised. While our *in vitro* assays examine the synthesis of a short 14nt product, *in vivo*, FluPol must processively synthesise between 890 nt and 2341 nt depending on the viral genome segment(19). Nsp7/8/12 in the SARS-CoV-2 replicase complex must synthesise even longer RNA products, up to 30 kilobases(7). Moreover, protein concentrations in the *in vitro* reactions may be higher than in cell culture systems. Together, these points mean that RNA synthesis inhibitors can show better efficacy *in vivo* than *in vitro*; for example, the nucleotide analogue remdesivir-triphosphate requires a concentration of 100 µM to inhibit SARS-CoV-2 nsp7/8/12 activity *in vitro*, but remdesivir has an IC_{50} of 0.77µM in cell culture(15, 20).

We find that SARS-CoV-2 nsp7/8/12 complex activity is inhibited by enisamium and VR17-04 with similar IC_{50} values to FluPol, 40.7mM and 2-3mM respectively (Fig 3C). This suggests that enisamium could inhibit SARS-CoV-2 growth, as it does for influenza virus, which can be confirmed by future studies; in particular, permission is currently being sought for a phase 3 clinical trial of enisamium iodide (Amizon® Max) in the treatment of COVID-19 in Ukraine. The rapid global spread of SARS-CoV-2 necessitates development of effective therapeutic interventions, and the most promising short-term strategy is to repurpose existing drugs. Our results demonstrate that enisamium, which is approved for use against influenza in 11 countries, inhibits RNA synthesis by the SARS-CoV-2 nsp7/8/12 complex. This raises the possibility that enisamium could be a viable therapeutic option against SARS-CoV-2 infection. A randomised, double-blind, placebo-controlled, parallel-group phase 3 trial will need to be used to assess the antiviral efficacy and safety of Amizon® in subjects with moderate Covid-19.

Materials and Methods

IAV in cell culture RNA synthesis assays

HEK 293T cells were transfected with plasmids expressing the subunits of the influenza A/WSN/33 (H1N1) virus RNA polymerase (pcDNA3-PB1, pcDNA3-PB2, pcDNA3-PA), the viral nucleoprotein (pcDNA3-NP) and a viral RNA template based on segment 5 (NP-encoding genome segment)(21, 22). As negative control, a PB1 active site mutant (PB1a) was used in which the active site SDD motif was mutated to SAA(23). GFP was expressed through transfection of pcDNA3-EGFP. Enisamium chloride (FAV00B) was added to the cell culture medium 15 min after transfection. Twenty-four hours after transfection, cells were washed in PBS and the total RNA extracted using Trizol and isopropanol precipitation. 5S rRNA, and IAV vRNA and mRNA steady state levels were subsequently analysed by radioactive primer extension and 6% denaturing PAGE as described previously(24). Phosphorimaging was performed on a Typhoon Scanner. GFP levels were measured in PBS on a SpectraMax plate reader.

IAV activity assays

The subunits of the A/WSN/33 (H1N1) influenza virus FluPol with a TAP-tag on PB2 (pcDNA3-PB1, pcDNA3-PB2-TAP, pcDNA3-PA) were expressed in HEK 293T cells and purified as heterotrimeric complex using IgG sepharose chromatography as described previously(25). Next, 0.5 mM CTP, 0.5 mM UTP, 0.05 mM ATP, 0.01 mM GTP, 0.5 mM ApG, 0.001 mM [α-^{32}P]GTP, FAV00A and VR17-04 at the concentrations indicated, and 0.5 μM 5' and 3' vRNA promoter strands were added to the purified RNA polymerase. After incubation at 30 degrees Celsius for 15 min, samples were analysed by 20% denaturing PAGE and autoradiography.

A549 cell extracts

A549 cells treated with FAV00A were lysed through sonication in 40 μl buffer A (10 mM Hepes pH 7.5, 0.1% NP-40, 150 mM NaCl, 5% glycerol, and 1 mM DTT) for 10 seconds. After centrifugation, extract was added to purified FluPol reactions as 1/10 of the total volume.

SARS-CoV-2 protein expression and purification

Full-length nsp7, nsp8, and nsp12 genes from SARS-CoV-2 were synthesized with codon optimization from IDT. The nsp12 gene was cloned into the MultiBac system, with a TEV cleavable protein-A tag on the C-terminus(26). The nsp7 and nsp8 genes were cloned into pGEX-6P-1 vector (GE Healthcare) with an N-terminal GST tag followed by a PreScission protease site. Nsp12 was expressed in Sf9 insect cells as previously described, nsp7 and nsp8 were expressed in E.coli BL21 (DE3) cells(27). Purification was started with affinity chromatography as previously described with minor modifications: all buffers were supplemented with 0.1 mM $MgCl_2$ and the NaCl concentration was changed to 300 mM(27). Nsp7 and nsp8 were purified with Glutathione Sepharose (GE Healthcare) instead of IgG. After overnight cleavage with TEV (nsp12) or PreScission (nsp7 and nsp8) proteases, the untagged proteins were further purified on a Superdex 200 (for nsp12) or Superdex 75 (for nsp7 and nsp8) Increase 10/300 GL column (GE Healthcare) using 25 mM HEPES–NaOH, pH 7.5, 300 mM NaCl and 0.1 mM $MgCl_2$. Fractions of target proteins were pooled, concentrated, and stored at 4°C.

SARS-CoV-2 nsp7/8/12 activity assays

Nsp7, nsp8 and nsp12 were mixed at a molar ratio of 2:2:1 and incubated overnight at 4°C to form the nsp7/8/12 complex. 40mer (5'-CUAUCCCCAUGUGAUUUUAAUAGCUUCUUAGGAGAAUGAC-3') and radiolabelled 20mer (5'-GUCAUUCUCCUAAGAAGCUA-3') RNAs corresponding to the 3' end of the SARS-CoV genome were pre-annealed by heating to 70°C for 5 mins followed by cooling to room temperature. 50nM pre-annealed RNA was incubated for 10-60 mins at 30°C with 500nM nsp7/8/12 complex, in reaction buffer containing 5 mM $MgCl_2$, 0.5mM of each ATP, UTP, GTP and CTP, 10mM KCl, 1U RNasin (Promega) and 1mM DTT. Assays in the presence of FAV00A or VR17-04 were run for 30 mins. Reactions were stopped by addition of 80% formamide and 10 mM EDTA, followed by heating to 95°C for 3 mins. Reaction products were resolved by 20% denaturing PAGE with 7M urea, and visualised by phosphorimaging on a Fuji FLA-5000 scanner. Data were analysed using ImageJ and Prism 8 (GraphPad).

Acknowledgments

Research in E.F.'s laboratory is supported by Medical Research Council program grant MR/R009945/1. A.P.W. is supported by Medical Research Council studentship 1960073. A.J.W.t.V is supported by joint Wellcome Trust and Royal Society grant 206579/Z/17/Z and the National Institutes of Health grant R21AI147172. J.M.G. is supported by Wellcome Investigator Award 200835/Z/16/Z.

All authors contributed to the design and conceptualisation of the work. A.P.W., A.J.W.t.V., H.F. and J.K. performed the experiments and analyzed the data. V.M. provided compounds. A.P.W. and A.J.W.t.V. wrote the paper with contribution from all authors.

Conflict of interest

V.M. is an employee of Farmak Public Joint Stock Company, Kiev, Ukraine. Part of this research was funded by Farmak Public Joint Stock Company, Kiev, Ukraine.

References

1. Krammer F, Palese P. 2015. Advances in the development of influenza virus vaccines. Nat Rev Drug Discov 14:167–182.

2. Gorbalenya AE, Baker SC, Baric RS, de Groot RJ, Drosten C, Gulyaeva AA, Haagmans BL, Lauber C, Leontovich AM, Neuman BW, Penzar D, Perlman S, Poon LLM, Samborskiy D V., Sidorov IA, Sola I, Ziebuhr J. 2020. The species Severe acute respiratory syndrome-related coronavirus: classifying 2019-nCoV and naming it SARS-CoV-2. Nat Microbiol. Nature Research.

3. Liu C, Zhou Q, Li Y, Garner L V., Watkins SP, Carter LJ, Smoot J, Gregg AC, Daniels AD, Jervey S, Albaiu D. 2020. Research and Development on Therapeutic Agents and Vaccines for COVID-19 and Related Human Coronavirus Diseases. ACS Cent Sci.

4. te Velthuis AJW, Fodor E. 2016. Influenza virus RNA polymerase: insights into the mechanisms of viral RNA synthesis. Nat Rev Microbiol 14:479–493.

5. Walker AP, Fodor E. 2019. Interplay between Influenza Virus and the Host RNA Polymerase II Transcriptional Machinery. Trends Microbiol 27:398–407.

6. Wu A, Peng Y, Huang B, Ding X, Wang X, Niu P, Meng J, Zhu Z, Zhang Z, Wang J, Sheng J, Quan L, Xia Z, Tan W, Cheng G, Jiang T. 2020. Genome Composition and Divergence of the Novel Coronavirus (2019-nCoV) Originating in China. Cell Host Microbe 27:325–328.

7. Ziebuhr J. 2005. The coronavirus replicase. Curr Top Microbiol Immunol 287:57–94.

8. Subissi L, Posthuma CC, Collet A, Zevenhoven-Dobbe JC, Gorbalenya AE, Decroly E, Snijder EJ, Canard B, Imbert I. 2014. One severe acute respiratory syndrome coronavirus protein complex integrates processive RNA polymerase and exonuclease activities. Proc Natl Acad Sci U S A 111:E3900–E3909.

9. te Velthuis AJW, Arnold JJ, Cameron CE, van den Worm SHE, Snijder EJ. 2009. The RNA polymerase activity of SARS-coronavirus nsp12 is primer dependent. Nucleic Acids Res 38:203–214.

10. Kirchdoerfer RN, Ward AB. 2019. Structure of the SARS-CoV nsp12 polymerase bound to nsp7 and nsp8 co-factors. Nat Commun 10:1–9.

11. Gao Y, Yan L, Huang Y, Liu F, Zhao Y, Cao L, Wang T, Sun Q, Ming Z, Zhang L, Ge J, Zheng L, Zhang Y, Wang H, Zhu Y, Zhu C, Hu T, Hua T, Zhang B, Yang X, Li J, Yang H, Liu Z, Xu W, Guddat LW, Wang Q, Lou Z, Rao Z. 2020. Structure of the RNA-dependent RNA polymerase from COVID-19 virus. Science.

12. Lehmann KC, Gulyaeva A, Zevenhoven-Dobbe JC, Janssen GMC, Ruben M, Overkleeft HS, Van Veelen PA, Samborskiy D V, Kravchenko AA, Leontovich AM, Sidorov IA, Snijder EJ, Posthuma CC, Gorbalenya AE. 2015. Discovery of an essential nucleotidylating activity associated with a newly delineated conserved domain in the RNA polymerase-containing protein of all nidoviruses. Nucleic Acids Res 43:8416–8434.

13. Shannon A, Tuyet Le NT, Selisko B, Eydoux C, Alvarez K, Guillemot J-C, Decroly E, Peersen O, Ferron F, Canard B. 2020. Remdesivir and SARS-CoV-2: structural requirements at both nsp12 RdRp and nsp14 Exonuclease active-sites. Antiviral Res 178:104793.

14. Chien M, Anderson TK, Jockusch S, Tao C, Kumar S, Li X, Russo JJ, Kirchdoerfer R, Ju J. 2020. Nucleotide Analogues as Inhibitors of SARS-CoV-2 Polymerase. bioRxiv.

15. Yin W, Mao C, Luan X, Shen D-D, Shen Q, Su H, Wang X, Zhou F, Zhao W, Gao M, Chang S, Xie Y-C, Tian G, Jiang H-W, Tao S-C, Shen J, Jiang Y, Jiang H, Xu Y, Zhang S, Zhang Y, Xu HE. 2020. Structural Basis for the Inhibition of the RNA-Dependent RNA Polymerase from SARS-CoV-2 by Remdesivir. bioRxiv.

16. World Health Organization. 2020. Table_of_therapeutics_Appendix_17022020.

17. EudraCT. 2013. EudraCT Number 2013-000301-23 - Clinical trial results - EU Clinical Trials Register.

18. Boltz D, Peng X, Muzzio M, Dash P, Thomas PG, Margitich V. 2018. Activity of enisamium, an isonicotinic acid derivative, against influenza viruses in differentiated normal human bronchial epithelial cells. Antivir Chem Chemother 26.

19. Nakatsu S, Sagara H, Sakai-Tagawa Y, Sugaya N, Noda T, Kawaoka Y. 2016. Complete and incomplete genome packaging of influenza A and B viruses. MBio 7.

20. Wang M, Cao R, Zhang L, Yang X, Liu J, Xu M, Shi Z, Hu Z, Zhong W, Xiao G. 2020. Remdesivir and chloroquine effectively inhibit the recently emerged novel coronavirus (2019-nCoV) in vitro. Cell Res 30:269–271.

21. Fodor E, Crow M, Mingay LJ, Deng T, Sharps J, Fechter P, Brownlee GG. 2002. A Single Amino Acid Mutation in the PA Subunit of the Influenza Virus RNA Polymerase Inhibits Endonucleolytic Cleavage of Capped RNAs. J Virol 76:8989–9001.

22. Fodor E, Devenish L, Engelhardt OG, Palese P, Brownlee GG, Garc A-sastre A. 1999. Rescue of Influenza A Virus from Recombinant DNA. J Virol 73:9679–9682.

23. Vreede FT, Jung TE, Brownlee GG. 2004. Model suggesting that replication of influenza virus is regulated by stabilization of replicative intermediates. J Virol 78:9568–72.

24. Robb NC, Smith M, Vreede FT, Fodor E. 2009. NS2/NEP protein regulates transcription and replication of the influenza virus RNA genome. J Gen Virol 90:1398–1407.

25. Deng T, Sharps J, Fodor E, Brownlee GG. 2005. In Vitro Assembly of PB2 with a PB1-PA Dimer Supports a New Model of Assembly of Influenza A Virus Polymerase Subunits into a Functional Trimeric Complex. J Virol 79:8669–8674.

26. Bieniossek C, Imasaki T, Takagi Y, Berger I. 2012. MultiBac: Expanding the research toolbox for multiprotein complexes. Trends Biochem Sci 37:49–57.

27. York A, Hengrung N, Vreede FT, Huiskonen JT, Fodor E. 2013. Isolation and characterization of the positive-sense replicative intermediate of a negative strand RNA virus. Proc Natl Acad Sci USA 110:E4238–E4245.

Table 1 List of compounds tested and their IC_{50} values. Compounds were provided by Farmak JSC. *Fold change relative to FAV00A. Ns = non-soluble. - = not tested.

COMPOUND	SOLVENT	IC_{50} REPLICATION	FOLD CHANGE IC_{50}*
FAV00A	DMSO	46.3 mM	1
VR16-01	DMSO	78.2 mM	0.6
VR17-01	Ns	-	-
VR17-02	Ns	-	-

VR17-03	DMSO	-	-
VR17-04	DMSO	0.84 mM	55
VR18-01	DMSO	34.2 mM	1.4
VR18-02	DMSO	94.8 mM	0.5
VR18-03	DMSO	74.01 mM	0.6
VR18-04	DMSO	35.16 mM	1.3

Figure Legends

Figure 1 Inhibition of FluPol by enisamium *in vitro*. A, Steady-state levels of IAV vRNA, 5S rRNA and GFP in the presence of enisamium. Gel shows primer extension analysis of 5S rRNA and IAV vRNA levels. A mutant IAV FluPol containing two amino acid substitutions in the PB1 active site (PB1a) was used as negative control. B, Chemical structures of enisamium iodide and VM17-04. C, Inhibitory effect of enisamium and VR17-04 on purified FluPol activity *in vitro*. D, Inhibition of purified FluPol activity by extracts from A549 cells treated with enisamium. Cells were treated with different amounts of enisamium and lysed in buffer A through sonication. Quantification is from n=3 independent reactions, and error bars represent standard deviation.

Figure 2 Purification and RNA synthesis activity of SARS-CoV-2 nsp7/8/12 complex. A, SARS-CoV-2 nsp7, nsp8 and nsp12 were expressed and purified from E. coli (nsp7 and nsp8) or Sf9 (nsp12) cells and visualised by SDS PAGE. B, Schematic of 40nt RNA template and 20nt radiolabelled primer. C, Purified nsp7/8/12 complex was tested for *in vitro* activity in the presence or absence of NTPs and RNA. The 20nt primer and 40nt product ran slightly slower than the markers, possibly due to differences in the RNA sequence or phosphorylation state. D, Quantification of 20nt primer extended by nsp7/8/12 at 10, 30 and 60 mins. Quantification is from n=3 independent reactions, error bars represent standard deviation.

Figure 3 Inhibition of SARS-CoV-2 nsp7/8/12 by enisamium and VR17-04. A, The effect of enisamium and VR17-04 on nsp7/8/12 *in vitro* activity was determined on a 40nt template. B, Relative activity of nsp7/8/12 was plotted against the concentration of enisamium and VR17-04 and dose-response curves were fit to the data. C, IC_{50} values of enisamium and VR17-04 for IAV FluPol and SARS-CoV-2 nsp7/8/12. The IC_{50} value for VR17-04 could not be calculated so was estimated. Quantification is from n=3 independent reactions, error bars represent standard deviation.

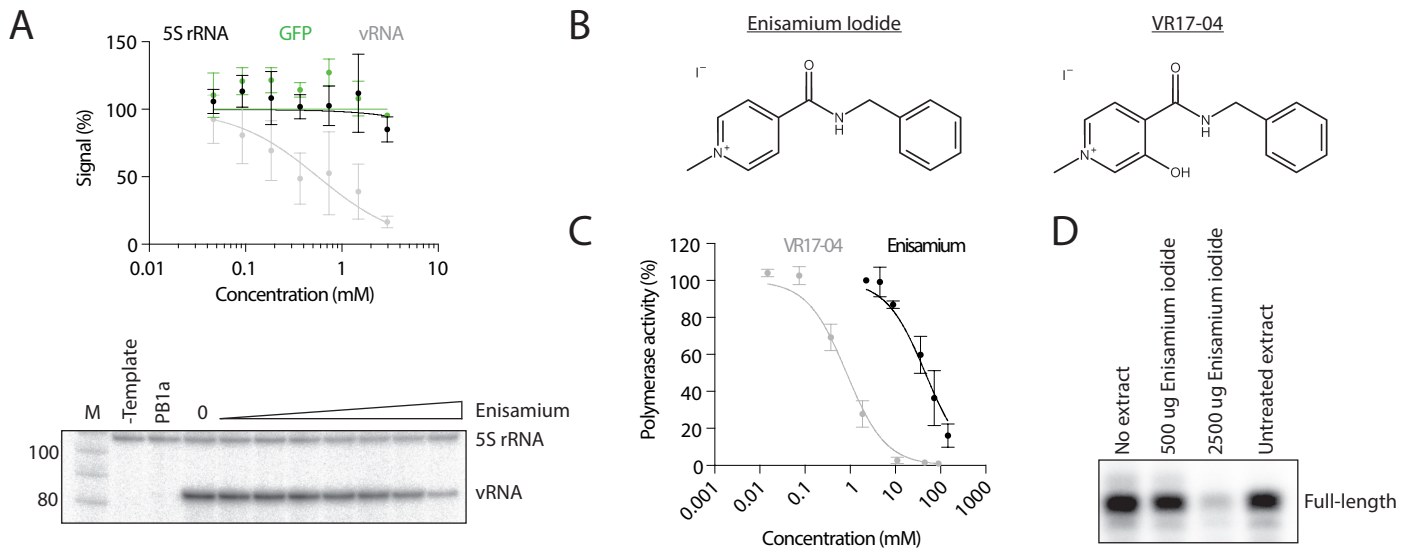
A
5S rRNA
GFP
vRNA
Signal (%)
150
100
50
0
0.01
0.1
1
10
Concentration (mM)
M
-Template
PB1a
0
Enisamium
5S rRNA
vRNA
100
80
B
Enisamium Iodide
VR17-04
I⁻
O
N
H
N⁺
OH
C
VR17-04
Enisamium
Polymerase activity (%)
120
100
80
60
40
20
0
0.001
0.01
0.1
1
10
100
1000
Concentration (mM)
D
No extract
500 ug Enisamium iodide
2500 ug Enisamium iodide
Untreated extract
Full-length

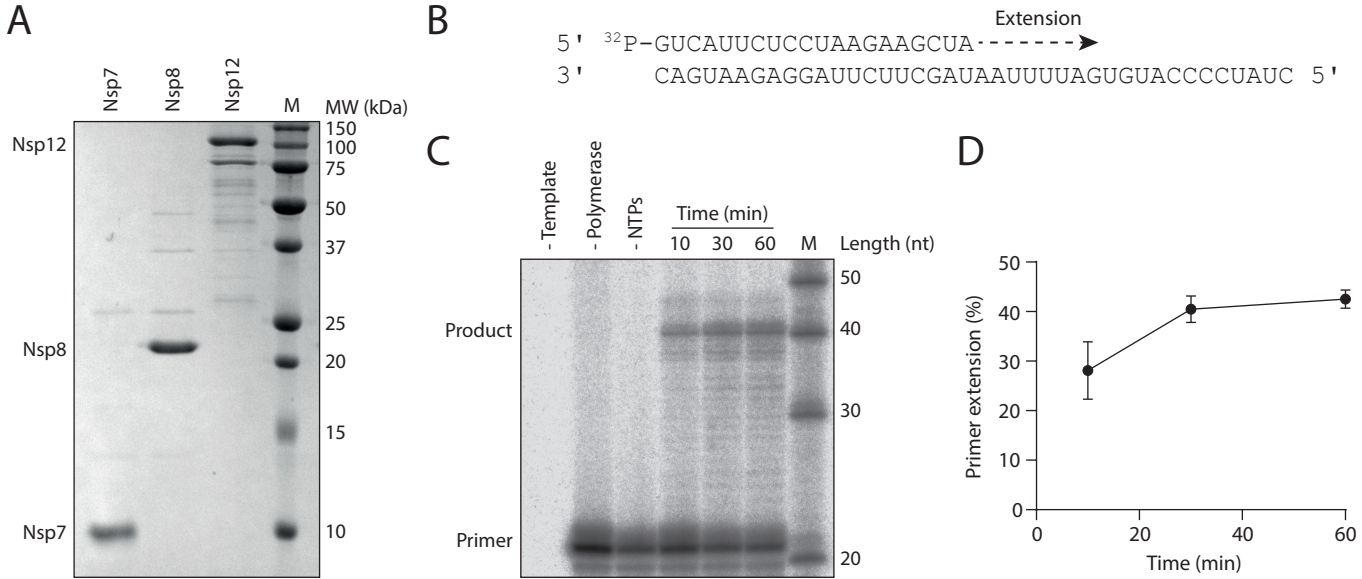
A
Nsp7
Nsp8
Nsp12
M
MW (kDa)
Nsp12
Nsp8
Nsp7
150
100
75
50
37
25
20
15
10
B
Extension
5' 32P-GUCAUUCUCCUAAGAAGCUA
3' CAGUAAGAGGAUUCUUCGAUAAUUUUAGUGUACCCCUAUC 5'
C
- Template
- Polymerase
- NTPs
Time (min)
10 30 60
M
Length (nt)
Product
Primer
50
40
30
20
D
Primer extension (%)
Time (min)
0
10
20
30
40
50
0
20
40
60

A

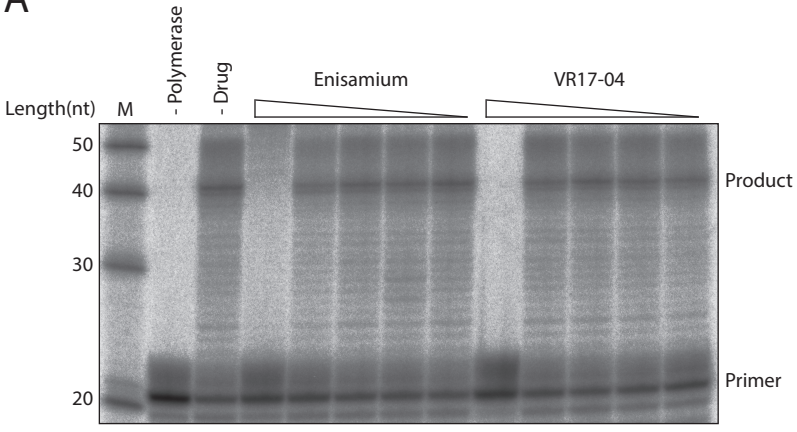

B

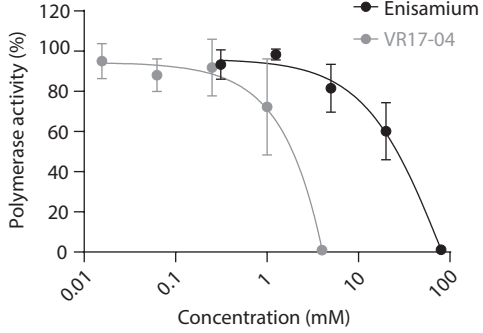

C

	IC_{50} (mM)	
	IAV	SARS-CoV-2
Enisamium	46.3	40.7
VR17-04	0.84	2.0 - 3.0